TJES
www.tj-es.com

Tikrit Journal of Engineering Sciences/Vol.20/No.4/ March 2013, (11-22)

A Contourlet-Based Image Denoising Technique with Coefficient Threshold Level Estimation.

Akram A. Dawood, Assistant Lecturer
Dept. of Computer Engineering – Mosul University

Received 25 July 2011; accepted 28 May 2012
Available online 18 April 2013

Abstract

In this paper, a new image denoising technique is proposed based on contourlet transform. Many random images are generated simulating the standard deviation level of the original noisy image and the contourlet threshold level is then calculated based on such simulations. Different contourlet coefficients are thresholded by such precalculated contourlet thresholds indicating a nonlinear thresholding manner. The resulting denoised images posses the superiority of the proposed technique over three other recents. Subjective and objective measurements of the proposed technique support such superiority.

Keywords: Contourlet Transform, Laplacian Pyramid, Directional Filter Banks and Random images.

تقنية لإزالة الضوضاء من الصور باعتماد الكونتورلت مع تخمين متكيف لمستوى حد العتبة في المعاملات.

الخلاصة

في هذا البحث تم اقتراح تقنية جديدة لإزالة الضوضاء من الصور باعتماد تحويل الكونتورلت.لقد تم توليد العديد من الصور العشوائية لمحاكاة مقدار الانحراف المعياري للصورة الأصلية الحاوية على الضوضاء.وتم بعد ذلك حساب مستوى حد العتبة الخاص بمركبات الكونتورلت وذلك بالاعتماد على تلك المحاكاة. إن مركبات الكونتورلت المختلفة قد تم إمرارها بحدود عتبة ذوات القيم المحسوبة مسبقاً من تلك المحاكاة مبينة طريقة غير خطية في استخدام حد العتبة. الصور الناتجة بعد عملية إزالة الضوضاء تظهر تفوق التقنية المقترحة على ثلاث تقنيات أخرى حديثة.إن القياسات الموضوعية وغير الموضوعية للتقنية المقترحة تؤكد ذلك التفوق.

الكلمات الدالة: تحويل كونتورلت وهرم لابلاس وأجراف المرشحات ألاتجاهية والصور العشوائية.

Introduction

During image formation, transmi-ssion and recording processes, images are deteriorated by noise. The purpose of image denoising is to reduce noise level while preserving principal signal features, such as edge contours and line details. Traditional denoising methods can be held in frequency domain or in spatial domain [1]. Studying and explo-iting the spatial properties of natural images have been one of the most important tasks in image processing. One key distinguishing feature of natural images is that they have intrinsic geometrical structures along object boundaries.

In 2002, M. N. Do and M. Vetterli [2] proposed the contourlet transform (CT) as a directional multi- resolution image representation that can efficiently capture and represent smooth object boundaries in natural images. The CT is constructed as a combination of the Laplacian pyramid (LP) and the directional filter banks (DFBs), where the LP iteratively decomposes a two-dimensional (2-D) image into low-pass and high-pass sub-bands, and the DFBs are applied to the high-pass sub-bands to further decompose the frequency spectrum, directionally. Using ideal filters, the CT will decompose the 2-D frequency spectrum into trapezoid-shaped regions [3].The CT is a new extension to wavelet transform (WT) in two dimensions using nonseparable and directional filter banks. With rich set of basis images oriented at varying directions in multiple scales, CT can effectively capture the smooth contours, which are the dominant features in natural images, with only a small number of coefficients [4].

It is well known that many signal processing tasks, such as compression, denoising, feature extraction and enhanc - ement, benefit tremendously from hav- ing a parsimonious representation of the signal at hand. The CT aimed at improving the representation sparsity of images over the WT. The main feature of contourlets is the potential to efficiently handle 2-D singularities, *i.e*. edges, unlike wavelets which can only deal with point singularities, exclusively. This difference is caused by following two main properties that the CT possesses:

1) The directionality property, *i.e.* having basis functions at many directions, as opposed to only 3 directions of wavelets.

2) The anisotropy property, meaning that the basic functions appear at various aspect ratios (depending on the scale), whereas wavelets are separable functions and thus their aspect ratio equals to 1. Due to its structural resemblance with the WT, many image processing tasks applied on wavelets can be seamlessly adapted to contourlets [5]. Figure 1 illustrates the difference between wavelet and contourlet transforms. 2-D WTs are only good at catching point discontinuities, but don't capture the geometric smoothness of the contours. The CT was improved for the solution of this problem. It can be seen from the Figure 1, wavelet transforms are the square transforms which can describe only point-wise discontinuances. But CTs are able to creep over the linear parts of contours and therefore, less number of coefficients for the suitable description of a continuous contour, are necessary. With such a rich set of bases functions, contourlets can represent a smooth contour with smaller number coefficients compared with wavelets [6]. Since the CT uses contour segments to realize the local, multi-resolutional and directional image expansions, hence it's named the contourlet transform [7].

Since 2005, many attempts were succeeded in illustrating the background theory, developments and applications of the CT [8]- [10]. Such transform was then utilized to perform image denoising by combining 2-D WT and nonsubsampled directional filter banks [11] and by employing a cycle spinning (CS) method to improve the denoising performance of its sharp frequency localization [12]. Image denoising based on contourlet- domain hidden Markov tree (CHMT) models were proved to achieve superior denoising results over wavelet-domain HMT (WHMT) models in terms of visual quality. But denoising by means of CHMT still introduces some artifacts due to the lack of translation invariance of the CT. It was noticed that employing a CS-based technique to develop trans- lation invariant CHMT denoising sche-me enhanced estimation results for images that are corrupted with additive Gaussian noise [13].

Recently, R. Sivakumar and G. Balaji, in 2009 used CT for speckle image denoising. This algorithm is more efficient than the wavelet algorithm in image denoising particularly for the removal of speckle noise.The parameters considered for comparing the wavelet and Contourlet Transforms are Signal -to -Noise Ratio (SNR) and Image Enhancement Factor (IEF), where IEF can be defined as the ratio between the square of difference between the noisy image and the original image to

the square of difference between the enhanced image and the reference image [3]. Also, Zuofeng Zhou, Jianzhong Cao and Weihua Liu in 2009, used a contourlet-based image denoising algorithm with adaptive windows which utilized both the captured directional information by the CT and the intrinsic geometric structure information of the image. The adaptive window in each of the Contourlet sub-band is first fixed by autocorrelation function of contourlet coefficients' energy distribution, and then the local Wiener filtering is used to denoise the noisy image [14]. Later in 2009, Xiaoyue Wu, *et al* presented an adaptive image denoising scheme by combining the nonsubsampled Contou-
rlet transform (NSCT) and total variation model. The original image is first decomposed using NSCT. Then the mean squared error (MSE) is estimated based on Stein's unbiased risk estimation (SURE). The noise of each decomposed sub-band is reduced using the linear adaptive threshold function, which can be constructed based on the MSE producing the preliminary primary denoised image after reconstruction. Then the preliminary primary denoised image is further filtered using the total variation model, producing the final denoised image [15].

More recently, Changhua Lu, Jie Shen, and Xiaoya Yu, in 2010 applied NSCT with translational invariance to image denoising which could capture the intrinsic geometrical structure of bottle image. After the scale of NSCT is determined, NSCT is used to transform the noisy image of glass bottle. A low frequency component and some high frequency components will be obtained. Through the use of the coefficients of high frequency components from different directions of the same scale, adaptive thresholds is obtained [16]. Also, in 2010 Zhe Liu and Huanan Xu proposed a novel image denoising algorithm using the CT and the two dimensional Principle Component Analysis (2-DPCA). The noise image can be decom-posed by the Contourlet into directional sub-bands. The 2-DPCA is then carried out to estimate the threshold for the image blocks in high frequency sub-bands. The soft thresholding shrinkage can hence be employed on the Contourlet coefficients without estimating the noise variance [17]. After that in the same year, N. Sugitha and S. Arivazhagan used many of the transformations for multiresolution analysis, such as WT, CT and NSCT for image denoising. In that work, different shrinkage rules such as Universal shrink, VISU shrink, Minimax shrink, SURE shrink, Bayes shrink, and Normal shrink were incorporated. These shrinkage rules combined with soft thresholding were applied to several Gaussian noise added test images [18].

In this paper, a new technique is introduced for denoising gray-scale images using CT. The standard deviation of an input noisy image is estimated by generating random images and applying the same CT coefficient in different levels on them. With the help of such criteria, the corresponding standard deviation is calculated, and the contou-
rlet threshold is found.

Contourlet Transform

Contourlet transform is a multi-scale and directional image representa-tion that uses first a wavelet like structure for edge detection, and then a local directional transform for contour segment detection. A double filter bank structure of the contourlet is shown in Figure 2 for obtaining sparse expansions for typical images having smooth contours. In the double filter bank structure, LP is used to capture the point discontinuities, and then followed by a DFB, which is used to link these point discontinuities into linear structures. The contourlets have elongated supports at various scales, directions and aspect ratios. This allows contourlets to efficie- ntly approximate a smooth contour at multiple resolutions. In the frequency domain, the CT provides multi-scale and directional decompositions [19].

1- Laplacian Pyramid (LP)

One way to obtain a multi-scale decomposition is to use the LP introduc-
ed by Burt and Adelson. The LP decomposition at each level generates a down sampled low-pass version of the original and the difference between the original and the prediction, resulting in a

band-pass image[2]. Figure 3(a) depicts this decomposition process, where *H* and *G* are called (low-pass) analysis and synthesis filters, respectively, and *M* is the sampling matrix. The process can be iterated on the coarse (down sampled low-pass) signal. It should be noted that in multidimensional filter banks, sampling is represented by sampling matrices; for example, down sampling $x[n]$ by M yields $x_d[n] = x[M_n]$, where M is an integer matrix. A drawback of LP is the implicit oversampling. However, in contrast to the critically sampled wavelet scheme, the LP has the distinguishing feature that each pyramid level generates only one band-pass image (even for multidimensional cases), and this image does not have "scrambled" frequencies. This frequency scrambling happens in the wavelet filter bank when a high-pass channel, after down sampling, is folded back into the low frequency band, and thus its spectrum is reflected [3]. In LP, this effect is avoided by down sampling the low-pass channel only by the use of the LP using the theory of frames and oversampled filter banks. It is shown that the LP with orthogonal filters (that is, the analysis and synthesis filters are time reversal, $h[n] = g[-n]$, and $g[n]$ is orthogonal to its translates with respect to the sampling lattice by M) provides a tight frame with frame bounds are equal to 1. The optimal linear reconstruction using the dual frame operator (or pseudo-inverse) is adopted as shown in Figure 3(b). Where the signal is obtained by simply adding back the difference to the prediction from the coarse signal [20].

2-Directional Filter Bank (DFB) Decomposition

DFB is designed to capture the high frequency content like smooth contours and directional edges. Several implementations of these DFBs are available in the literature [19]. This DFB is implemented using a *k*- level binary tree decomposition that leads to 2^k directional sub- bands with wedge shaped frequency partitioning as shown in Figure 4. A simplified DFB structure is adopted here. It is constructed from two building blocks. The first one is a two-channel quincunx filter bank with fan filters see Figure 5. It divides the 2-D spectrum into two directions, horizontal and vertical. The second one is a shearing operator, which amounts to the reordering of image pixels. Due to these two operations, directional information is preserved.

Figure 6 shows an application of a shearing operator where a -45° direction edge becomes a vertical edge. By adding a pair of shearing operator and its inverse (" unshearing") to before and after, respectively, the two channel filter bank in Figure 5, a different directional frequency partition can be obtained while maintaining perfect reconstruction. Thus, the key in the DFB is to use an appropriate combination of shearing operators together with two-direction partition of quincunx filter banks at each node in a binary tree-structured filter bank, to obtain the desired 2-D spectrum division as shown in Figure 4 [20].

Combination of a LP and DFB gives a double filter bank structure known as contourlet filter bank. Band pass images from the LP are fed to DFB so that directional information can be captured. The scheme can be iterated on the coarse image. Decomposing it into directional sub-bands at multiple scales [19].

The proposed technique

The flow chart of the proposed technique is shown in Figure 7. The noisy image is read first, where the noise may be an additive (such as Additive White Gaussian Noise (AWGN)),or multiplicative (speckle noise). Then, a scaled version of the standard deviation (σn) of the noisy image is computed.

'9-7' and 'pkva' filters are used in pyramidal decomposition that represent the LP and directional decomposition that represent the DFB, respectively. The same filters are used for reconstruction. The number of directional filter bank decomposition levels (n leaves, or nlevs) is then selected. That means vector of number of directional filter bank decomposition levels at each pyramidal level (from coarse to fine scale) is fixed. The output of contourlet decomposition will contain a cell vector of length [length (nlevs)+1]. Each cell corresponds to one pyramidal level is a cell vector that contains band-pass

directional sub-bands from the DFB at that level. As a result of above analysis, the contourlet coefficients will be obtained. These coefficients are converted to a vector form using the 2-D to 1-D matlab transformation is added to the matlab program.

$$[A] = Y(:) \quad \ldots\ldots(1)$$

Where Y is an output of the PDFB. Instruction (1) converts the contourlet coefficients into a vector form and then stores the results of conversion on into a matrix denoted as [A], where A represents a 1-D vector array that contains all PDFB coefficients. The estimation of the noise standard deviation in the PDFB domain is accomplished. The idea is to generate random images to estimate the noise standard deviation using the same contourlet coefficients that is applied on the noisy images in different levels. A first random image of the same size of the input noisy image is generated. Its contourlet coefficients are then obtained and converted to a vector like A. This operation is repeated for many other random images to find other A matrix. The average noise standard deviation (σ_r) is then calculated for all those random images. Such (σ_r) is then stored in another matrix that will be used for evaluating matrix containing the contourlet thresholds (C_{th}), where

$$C_{th} = \sigma_n * \sigma_r \quad \ldots\ldots(2)$$

Where * denotes a scalar to matrix multiplication.

Our experiments indicate that ten random images can be used to serve for such purpose. If this number of random images is increased to 100, then both SNR and PSNR will be improved slightly, but on behave of the execution time. If less than 10 random images is used, then both SNR and PSNR will be decreased, with no efficient improve-ment in the execution time.

The final contourlet threshold (C_{th}) is computed by equating the average standard deviation level of these ten random images with the standard deviation of the input noisy image. These (C_{th}) levels are then compared with the all elements of A matrix on base of element by element as given by the equation:-

$$A_i = \begin{cases} A_i & \text{for } A_i > C_{th} \\ 0 & \text{otherwise} \end{cases} \quad \ldots\ldots(3)$$

Where A_i is an element in the matrix A.

This scanning represents a nonlinear thresholding method. The final step is to convert the resulting vector after thresholding to contourlet coeffici-ent to obtain a reconstructed image which is the denoised one. As shown in Figure 7.

Results and Comparisons

In this paper, the denoising performance of the proposed technique is compared with other algorithms in references [3], [17], and [18], using the contourlet coefficient threshold level estimation. Tables 1, 2 and 3 contain the values of both PSNR and SNR (in dB) of the denoised images using the proposed technique and others for comparison purpose. Table 1 illustrates the superior-ity of the proposed technique in speckle noise reduction of noisy Lena, Pepper, and Barbara gray-scale images (with different noise levels) as compared to the algorithm in reference [3]. As seen, the SNR values (in dB) are more in the proposed technique. The resulting denoi- sed Lena image is shown in Figure 8.

The proposed technique is also compared with the algorithms in reference [17] and [18] for AWGN denoising of Pepper and Barbara images. The corresponding PSNR values (in dB) are illustrated in Table 2, highlighting that the proposed technique is also superior for different noise levels. The resulting denoised images are shown in Figure 9 for pepper images (with σ_n =30). For more judgments on the propo- sed technique in high noise levels, it is finally compared with the nonsubsampled CT algorithm best results given in reference [18].Which accedes CT in denoising, the resulting PSNR values (in dB) are summarized in Table 3 for σ_n in the range of 10 to 50 for the prementioned

images. Figure 10 shows the resulting denoised images of Barbara for the technique in reference [18] and the proposed one.

Conclusions

A new image denoising technique has been proposed utilizing random images simulation of the original noisy image. The technique has been based on the idea of the estimation of the level contourlet thresholding. Which encounters for the simulation outputs in its evaluations. The resulting denoised images have been compared with three other recent techniques.

The comparisons highlight that the proposed technique is superior for both types of noise (speckle and AWGN). It has been proved that the proposed technique is also still effective in denoising images with high-level noise.

References

1. Q. Zhao, X. Wang, B. Ye, and D. Zhou, " Mixed image denoising method of non-local means and adaptive bayesian threshold estimation in NSCT domain", 3rd IEEE International Conference on Computer Science and Information Technology (ICCSIT), Vol.6, pp. 636-639, 9-11 July 2010.
2. B. Li, X. Li, S. Wang, and H. Li; , " A Multiscale and Multidirectional Image Denoising Algorithm Based on Contourlet Transform", International Conference on Intelligent Information Hiding and Multimedia Signal Processing (IIH-MSP '06).pp. 635-638, Dec. 2006.
3. R. Sivakumar, G.Balaji, R. Ravikiran, R. Karikalan, and S. Janaki," Image Denoising using Contourlet Transform", Second International Conference on Computer and Electrical Engineering, (ICCEE '09). Vol.1, pp. 22-25, 28-30 Dec. 2009.
4. Po, D.D.-Y, and Do, M.N," Directional multi-scale modeling of images using the contourlet transform". IEEE Transactions on Image Processing, Vol.15, No.6, pp. 1610-1620, June 2006.
5. B. Matalon, M. Elad, and M. Zibulevsky, "Image denoising with the contourlet transform". In Proceedings of SPARSE'05, Rennes, France, Nov. 2005.
6. A. Altun, and N. Allahverd, " Recognition of fingerprints enhanced by contourlet transform with artificial neural networks", 28th International Conference on Information Technology Interfaces (ITI), pp. 167-172, Croatia, 19-22 June 2006.
7. Y. Yan, and L. Osadciw, "Contourlet Based Image Recovery and De-noising Through Wireless Fading Channels", Conference on Information Science and Systems, The Johns Hopkins University, 16-18 March 2005.
8. R. Eslami, and H. Radha, " Image denoising using translation-invariant contourlet transform", IEEE International Conference on Acoustics, Speech, and Signal Processing Proceedings. (ICASSP '05). Vol.4, pp. 557- 560, 18-23 March 2005.
9. R. Eslami, and H. Radha, " Optimal Linear Combination of Denoising Schemes for Efficient Removal of Image Artifacts", IEEE International Confere-nce on Multimedia and Expo, pp. 465-468, 9-12 July 2006.
10. B. Song, L. Xu, and W. Sun, "Image Denoising Using Hybrid Contourlet and Bandelet Transforms", Fourth Internati-onal Conference on Image and Graphics (ICIG). pp. 71-74, 22-24 Aug. 2007.
11. Z. Liu, and H. Xu, "Image Denoising with Nonsubsampled Wavelet-Based Contourlet Transform", Fifth International Conference on Fuzzy Systems and Knowledge Discovery (FSKD'08). pp. 301-305, 18-20 Oct. 2008.
12. Q. Xiaobo, and Y. Jingwen, " The cycle spinning-based sharp frequency localized contourlet transform for image denoising", 3rd International Conference on Intelligent System and Knowledge Engineering (ISKE) , pp. 1247-1251, 17-19 Nov. 2008.
13. K. Li,W. Wang, and J. Gao, " Image Denoising Based on Contourlet-Domain HMT Models Using Cycle

Spinning", 2008 International Conference on Computer Science and Software Engineering, pp.162-165, 12-14 Dec. 2008.

14. Z. Zhou, J. Cao, and W. Liu, "Contourlet-based image denoising algorithm using adaptive windows", 4th IEEE Conference on Industrial Electro-nics and Applications (ICIEA).pp. 3654-3657, 25-27 May 2009.
15. X. Wu, B. Guo, S. Qu, and Z. Wang, "A New Adaptive Image Denoising Method Combining the Nonsubsampled Contourlet Transform and Total Variation", Fifth International Conference on Information Assurance and Security (IAS '09). pp. 581-584, 18-20 Aug. 2009.
16. C. Lu, J. Shen, and X. Yu, " Bottle image de-noising using adaptive threshold based on nonsubsampled contourlet transform", 2nd International Conference on Signal Processing Systems (ICSPS), pp. 792-795, 5-7 July 2010.
17. Z. Liu, and H. Xu, "Image denoising using Contourlet and two-dimensional Principle Component Analysis", International Conference on Image Analysis and Signal Processing (IASP), pp. 309- 313, 9-11 April 2010.
18. N.Sugitha, S. Arivazhagan, " Performance analysis of multiresolution image denoising schemes", IEEE International Conference on Communi- cation Control and Computing Technologies (ICCCCT), pp. 413-418, 7-9 Oct. 2010.
19. Ch. Srinivasa rao , S. Srinivas kumar and B.N.Chatterji, " Content Based Image Retrieval using Contourlet Transform", ICGST-GVIP Journal, Vol. 7, pp. 9- 15, Nov. 2007.
20. M. Do, M.Vetterli, "The contourlet transform: an efficient directional multiresolution image representation", IEEE Transactions on Image Processing, Vol.14, No.12, pp. 2091-2106, Dec. 2005.
21. Y. Tanaka, M. Ikehara, and T. Nguyen," Multiresolution Image Repres-entation Using Combined 2-D and 1-D Directional Filter Banks", IEEE Transactions on Image Processing, Vol.18, No.2, pp. 269-280, Feb. 2009.

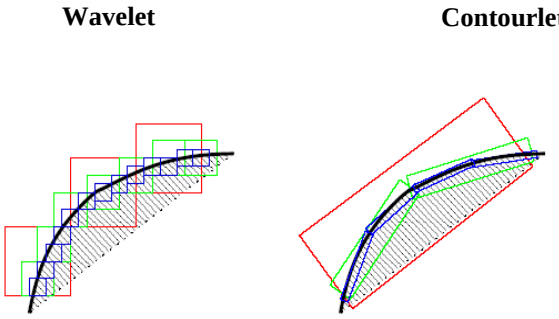

Figure (1) Wavelet vs. contourlet transform.

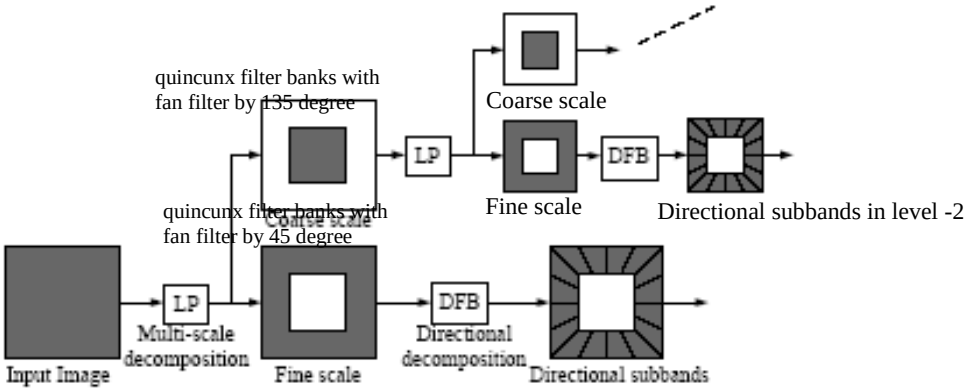

Figure (2) Block diagram of Contourlet transform.

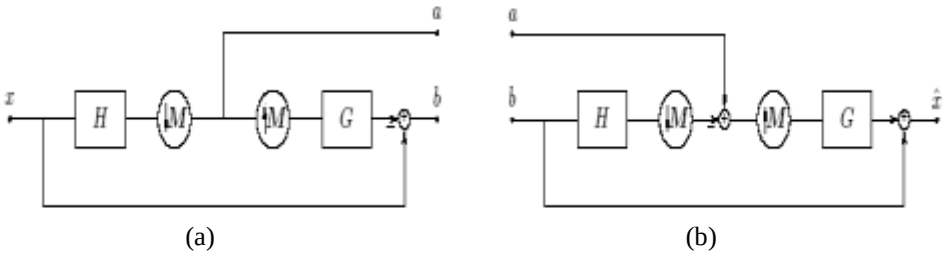

Figure (3) Laplacian pyramid. (a) One level of decomposition. The outputs are a coarse approximation a[n] and a difference b[n] between the original signal and the prediction. (b) The new reconstruction scheme for the Laplacian pyramid.

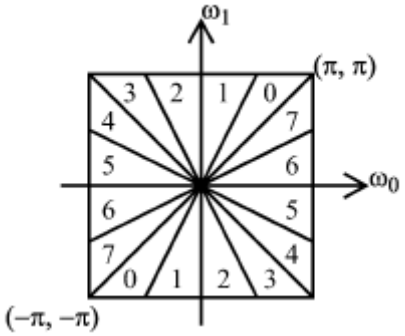

Figure (4) DFB Frequencies Partitioning, after [21].

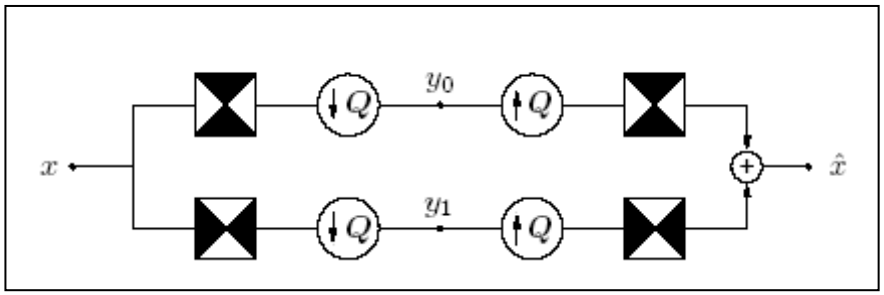

Figure (5) 2-D spectrum partition using quincunx filter banks with fan filters. The black regions represent the ideal frequency supports of each filter. Q is a quincunx sampling matrix.

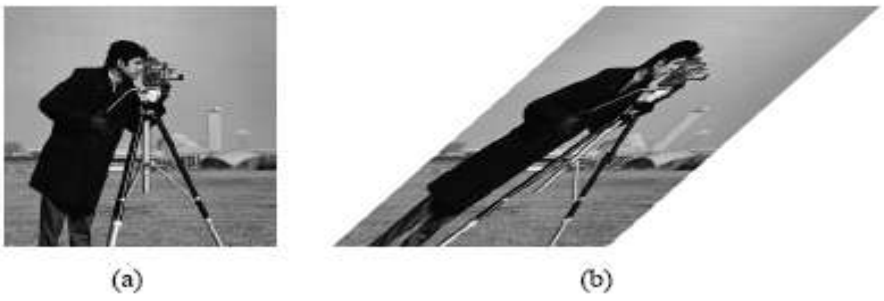

Figure (6) Example of shearing operation that is used like a rotation operation for DFB decomposition. (a) The "cameraman" image. (b) The "cameraman" image after a shearing operation.

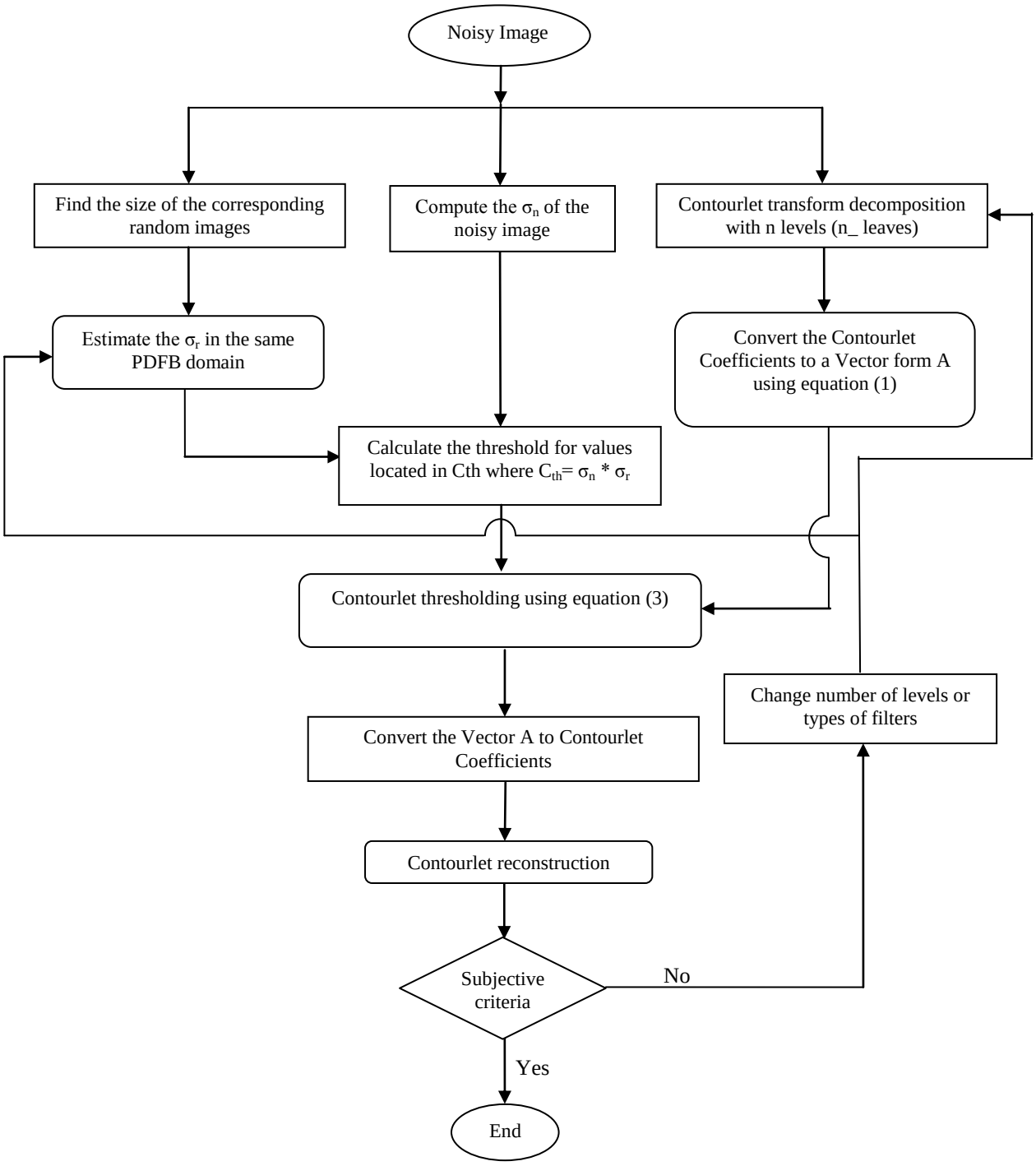

Figure (7) Flow chart of the proposed technique.

a) Noisy image

b) Denoised image for the algorithm in [3].

c) Denoised image for the proposed technique.

Figure (8) Denoising results of Lena image (Speckle Noise Variance= 0.1).

a) Noisy image

b) Denoised image for the algorithm in [17]

c) Denoised image for the proposed technique

Figure (9) Denoising results of peppers image (AWGN σ_n = 30).

a) Noisy image

b) Denoised image for the algorithm in [18]

c) Denoised image for the proposed technique

Figure 10 Denoising results of Barbara image (AWGN σ_n= 30).

Table (1)

Test Images	SNR(dB)	
	Proposed algorithm using Contourlet[3]	The proposed technique
	NOISE LEVEL= 0.03dB	
Lena	11.77	**14.515**
Peppers	11.36	**14.762**
Barbara	9.81	**13.971**
	NOISE LEVEL= 0.04dB	
Lena	10.95	**13.550**
Peppers	10.68	**13.784**
Barbara	9.39	**13.159**
	NOISE LEVEL= 0.06dB	
Lena	10.01	**12.152**
Peppers	9.65	**12.382**
Barbara	8.67	**11.989**
	NOISE LEVEL= 0.1dB	
Lena	8.20	**10.415**
Peppers	8.56	**10.689**
Barbara	7.66	**10.456**

Table (2)

Test Images	Noise Type	Noise Variance	method proposed in[17]	the proposed technique
Peppers	AWGN	10	31.96	**34.01**
		15	30.36	**33.55**
		20	29.20	**33.23**
		25	28.16	**32.99**
		30	27.55	**32.81**
Barbara		10	30.34	**33.80**
		15	27.90	**33.45**
		20	26.82	**33.17**
		25	25.90	**32.95**
		30	25.11	**32.78**

Table (3)

Test Images	σ_n of AWGN	NSCT in [18]	The Proposed technique
Barbara	10	30.1185	**36.922**
	20	28.2857	**34.011**
	30	25.5475	**33.494**
	40	22.5863	**33.188**
	50	20.2459	**33.061**
Lena	10	31.3411	**35.335**
	20	29.0793	**34.233**
	30	25.7695	**33.481**
	40	22.8239	**33.112**
	50	20.3428	**32.885**
Peppers	10	30.5185	**36.881**
	20	28.5624	**34.049**
	30	25.5915	**33.570**
	40	25.5915	**33.269**
	50	20.2599	**33.071**